

Color Octet Scalar Bound States at the LHC

Chul Kim^{*1} and Thomas Mehen^{†1}

¹*Department of Physics, Duke University, Durham, NC 27708*

Abstract

One possible extension of the Standard Model scalar sector includes $SU(2)_L$ doublet scalars that are color octets rather than singlets. We focus on models in which the couplings to fermions are consistent with the principle of minimal flavor violation (MFV), in which case these color octet scalars couple most strongly to the third generation of quarks. When the Yukawa coupling of color octet scalars to Standard Model fermions is less than unity, these states can live long enough to bind into color-singlet spin-0 hadrons, which we call octetonia. In this paper, we consider the phenomenology of octetonia at the Large Hadron Collider (LHC). Predictions for their production via gluon-gluon fusion and their two-body decays into Standard Model gauge bosons, Higgs bosons, and $t\bar{t}$ are presented.

^{*} Electronic address: chul@phy.duke.edu

[†] Electronic address: mehen@phy.duke.edu

A major goal of the physics program at the Large Hadron Collider (LHC) is to experimentally probe the mechanism of electroweak symmetry breaking. Although electroweak symmetry breaking can be accomplished by the Higgs mechanism with a scalar doublet transforming in the $(\mathbf{1}, \mathbf{2})_{1/2}$ representation of the $SU(3) \times SU(2)_L \times U(1)_Y$ gauge group, it is possible that a scalar sector with a richer structure will be revealed at the LHC. An important constraint on an extended scalar sector comes from the absence of flavor changing neutral currents. A natural way to ensure that theories of new physics are consistent with these constraints is to invoke the principle of Minimal Flavor Violation (MFV) [1, 2]. MFV requires that the Standard Model Yukawa matrices are the sole source of the violation of the $SU(3)^5$ flavor symmetry that would be present in the absence of fermion mass terms. If one invokes MFV as a guiding principle for models of new physics, possible extensions of the scalar sector are very highly constrained. Besides the Standard Model Higgs field, only scalars in $(\mathbf{8}, \mathbf{2})_{1/2}$ representation can have Yukawa couplings that are consistent with MFV [3].

Color-octet scalars also arise in $SU(5)$ grand unified theories if the fundamental theory contains scalars in the $\mathbf{45}$ of $SU(5)$ [4, 5, 6]. Higgs fields in this representation are invoked in many $SU(5)$ models to obtain a realistic fermion mass spectrum. In adjoint $SU(5)$ GUT's, color octet scalars are actually required to be light ($\lesssim 100$ TeV) in order to obtain unified couplings [5, 6]. Color octet scalars can also arise in theories of Pati-Salam unification [7, 8] as well as cosmological models of dark energy [9].

All of this motivates serious consideration of the collider signals of color octet scalars. The LHC phenomenology of color octet scalars has been studied recently in Refs. [10, 11]. In order to be consistent with MFV, the Yukawa couplings of these color octet scalars to Standard Model fermions must be [3]

$$\mathcal{L} = -\eta_U g_{ij}^U \bar{u}_{Ri} T^A Q_{Lj} S^A - \eta_D g_{ij}^D \bar{d}_{Ri} T^A Q_{Lj} S^{A\dagger}, \quad (1)$$

where

$$S^A = \begin{pmatrix} S^{A+} \\ S^{A0} \end{pmatrix} \quad (2)$$

are the color octet scalars, Q_{Lj} is the Standard Model $SU(2)_L$ doublet of quarks, u_R and d_R are the right-handed Standard Model quark fields, $g_{ij}^{U,D} = \sqrt{2} M_{ij}^{U,D}/v$, where $M_{ij}^{U,D}$ are the Standard Model quark mass matrices and $v/\sqrt{2}$ is the vacuum expectation value of the Higgs doublet. In addition to the Yukawa couplings listed above the scalar octets have gauge couplings to Standard Model gauge bosons, and there is a scalar potential which allows for scalar octet self-interactions as well as scalar octet couplings to the Standard Model Higgs [3]. In general, there are three mass eigenstates, $S^{A\pm}$, $S_R^{A0} = \sqrt{2} \operatorname{Re} S^{A0}$, and $S_I^{A0} = \sqrt{2} \operatorname{Im} S^{A0}$,

with masses given by

$$\begin{aligned} m_{S^\pm}^2 &= m_S^2 + \lambda_1 \frac{v^2}{4} \\ m_{S_R^0}^2 &= m_S^2 + (\lambda_1 + \lambda_2 + 2\lambda_3) \frac{v^2}{4} \\ m_{S_I^0}^2 &= m_S^2 + (\lambda_1 + \lambda_2 - 2\lambda_3) \frac{v^2}{4}, \end{aligned} \quad (3)$$

where m_S , λ_1 , λ_2 , and λ_3 are parameters appearing in the scalar potential. If custodial $SU(2)$ symmetry is imposed on the potential, $\lambda_2 = 2\lambda_3$, and the $S^{A\pm}$ and S_I^{A0} are degenerate.

If η_U and η_D are both order unity, the dominant decays of the S^A are $S^{A+} \rightarrow t\bar{b}$ and $S_{R,I}^{A0} \rightarrow t\bar{t}$, or $S_{R,I}^{A0} \rightarrow b\bar{b}$, if the $S_{R,I}^{A0}$ mass lies below $2m_t$. In this case, to search for color octet scalars, one would look for modifications to Standard Model predictions for final states with multiple heavy flavor jets. Ref. [11] obtained a lower bound of ~ 200 GeV for the color octet masses by studying the process $gg \rightarrow S^A S^A \rightarrow b\bar{b}b\bar{b}$, which is constrained by the CDF search for $H \rightarrow b\bar{b}$ plus associated b jets in Ref. [12].

In this paper we investigate the possibility of producing color singlet bound states of these color octet scalars, which we will call octetonia. For this to occur, the scalar octet must live long enough so that it has time to form a bound state prior to decaying. For example, we have observed top quarks in hadron colliders, but not toponium resonances because the top quark decays too quickly. If they exist, octetonia are heavy enough that they can be reasonably modelled as quasi-Coulombic bound states, therefore the binding energy of the ground state octetonium is expected to be $\approx m_S N_c^2 \alpha_s^2(m_S v)/4$, where m_S is the color octet scalar mass, N_c is the number of colors, and v is the typical velocity of the scalar in the bound state.¹ The factor N_c appears here because it is the color factor in the Coulomb potential for two particles in the **8** representation. If τ_{form} is the time scale for formation of the bound state (after the S^A pair has been produced), and τ_{life} is the lifetime of the two particle state, then, using the decay widths for $S^{A+} \rightarrow t\bar{b}$ calculated in Ref. [3] we find for bound states of $S^{A\pm}$,

$$\frac{\tau_{\text{form}}}{\tau_{\text{life}}} = \frac{2\Gamma[S^{A+}]}{B.E.} \sim 0.08 |\eta_U|^2 - 0.6 |\eta_U|^2, \quad (5)$$

for m_{S^\pm} in the range $200 - 500$ GeV. Here $B.E.$ is the binding energy. For comparison, the corresponding ratio for top quarks yields $\tau_{\text{form}}/\tau_{\text{life}} \approx 3$. For bound states containing neutral scalars, $\tau_{\text{form}}/\tau_{\text{life}}$ depends strongly on $m_{S_R^0}$ and $m_{S_I^0}$. If both masses are below the

¹ The typical velocity of the constituents of a quasi-Coulombic bound state of octets in QCD is estimated by demanding $v = N_c \alpha_s(m_S v)$ [13], which, for the one-loop expression for α_s , is solved by

$$v = \frac{2N_C \pi}{\beta_0 w[2N_c \pi m_S / (\beta_0 \Lambda_{\text{QCD}})]}, \quad (4)$$

where $w[x]$ is the Lambert W (or Product Log) function. For $m_S = 200 - 1200$ GeV, we find $v = 0.37 - 0.30$ and $\alpha_S(m_S v) = 0.12 - 0.10$.

$t\bar{t}$ threshold, 342 GeV, the $S_{R,I}^{A0}$ must decay to $b\bar{b}$ and then $\Gamma[S^{A0}]$ is suppressed by $(m_b/m_t)^2$ and $\tau_{\text{form}}/\tau_{\text{life}} \sim 6 \times 10^{-4}|\eta_D|^2$. In this scenario bound states clearly can form if η_D is of order unity. For $m_{S_{R,I}^0}$ above 400 GeV, the estimate for $\tau_{\text{form}}/\tau_{\text{life}}$ is similar to Eq. (5). In any case, we see that when $\eta_U < 1$ the criterion for bound state formation is satisfied.

Ref. [10] studied the impact of one loop diagrams with virtual color octet scalars on the Standard Model prediction for $R_b = \Gamma[Z^0 \rightarrow b\bar{b}]/\Gamma[Z^0 \rightarrow \text{hadrons}]$. Their results give an upper bound on η_U as a function of m_{S^\pm} . For $m_{S^\pm} = 200$ GeV the 1σ (2σ) upper bound is $|\eta_U| < 0.34$ ($|\eta_U| < 0.79$), while for $m_{S^\pm} = 500$ GeV the upper bound is $|\eta_U| < 0.62$ ($|\eta_U| < 1.45$), so for color octet scalars whose masses lie just beyond the existing upper bounds, the Yukawa coupling η_U will be small enough to accommodate the production of octetonia.

Like the S^A themselves the octetonia will decay into heavy quarks. However, the bound states can also decay via annihilation, much like conventional quarkonium states. The decays we focus on here are the decays to two gauge bosons: gg , $\gamma\gamma$, W^+W^- , γZ^0 , and Z^0Z^0 . Since the couplings of S^A to gauge bosons are fixed entirely by gauge invariance, calculation of these decay rates is model independent up to a universal factor, $|\psi(0)|^2$, the wave function at the origin squared. This sets the normalization of decay rates and cross sections, and can be crudely estimated in the quasi-Coulombic approximation. Thus the production cross section (as a function of the octetonium mass) can be estimated to within a factor of order unity. Furthermore, the relative branching fractions for the two-body decays to Standard Model gauge bosons can be reliably calculated. We also calculate the octetonia decays to Higgs boson pairs and to $t\bar{t}$. These decays are sensitive to the Yukawa couplings of the color octet scalars as well as parameters appearing in the color octet scalar potential.

In this paper we will focus on the production and decay of the three octetonia which can be produced directly via gluon-gluon fusion. These are O_+^0 , O_R^0 , and O_I^0 , which are color-singlet bound states of $S^{A+}S^{A-}$, $S_R^{A0}S_R^{A0}$, and $S_I^{A0}S_I^{A0}$, respectively. Many other bound states are possible, for example, O_R^+ which is a boundstate of $S^{A+}S_R^{A0}$ or O_{RI}^0 which is a bound state of $S_R^{A0}S_I^{A0}$. These octetonia can be produced in association with electroweak gauge bosons, for example, $gg \rightarrow O_R^+W^-$ or $gg \rightarrow O_{RI}^0Z^0$. These states cannot decay into two gluons which is the dominant annihilation decay mode for O_+^0 , O_R^0 , and O_I^0 . Therefore, octetonia such as O_R^+ or O_{RI}^0 may appear as two-body resonances in final states with three electroweak bosons which could make for interesting signals at the LHC. We leave the study of the production and decay of these octetonia to future work.

For the O_+^0 , O_R^0 , and O_I^0 , we consider only the production of the lowest radial excitation of the S -wave color singlet state. The wave function at the origin squared for a state with principal quantum number n will scale as $1/n^3$ so production cross sections for radially excited states will be correspondingly suppressed. This is also true for partial waves other than S -waves. From our calculation of $pp \rightarrow O_+^0 \rightarrow \gamma\gamma$, we expect that octetonia will form narrow resonances that will exceed Standard Model background if m_S lies in the range 200 - 500 GeV, corresponding to octetonia with masses from 400 - 1000 GeV, so we focus on this mass range in this paper. Nonobservation of resonances in $\gamma\gamma$, W^+W^- , Z^0Z^0 , etc., in this mass range will significantly increase existing lower bounds on the color octet scalar masses. In our calculations we will take $m_O = 2m_S$, neglecting the binding energies which

are expected to be of about 6 (for $m_O = 400$ GeV) to 16 GeV (for $m_O = 600$ GeV) in the quasi-Coulombic approximation. (Calculations of superheavy color-octet quarkonium binding energies in a realistic potential model yield similar estimates [14].) This $\sim 1.5\%$ shift in the mass of the octetonium will not significantly affect our predictions for production cross sections or decay rates.

The amplitude for the decay $O^+ \rightarrow GG'$, where G and G' are Standard Model gauge bosons, is obtained by convolving the amplitude for $S^{A+}S^{B-} \rightarrow GG'$ with the wavefunction of the octetonium state, which is

$$|O_+^0(P)\rangle = \frac{\delta^{AB}}{\sqrt{N_c^2 - 1}} \sqrt{\frac{2}{m_O}} \int \frac{d^3 k}{(2\pi)^3} \tilde{\psi}(k) |S^{A+}(P/2 + k)S^{B-}(P/2 - k)\rangle, \quad (6)$$

for O_+^0 . A similar definition holds for O_R^0 and O_I^0 . Here P^μ is the four-momentum of O_+^0 , k^μ is the relative momentum of the S^A within the bound state, and $\tilde{\psi}(k)$ is the momentum space wavefunction. The prescription for computing the production or decay is analogous to standard calculations of quarkonium production or decay. For decays of O_+^0 , one computes the amplitude for $S^{A+}(P/2 + k)S^{B-}(P/2 - k) \rightarrow X$, where X is the final state, and then convolves this amplitude with the wavefunction in Eq. (6). Since $P^0 \sim \mathcal{O}(m_O)$ but $k^\mu \sim \mathcal{O}(m_S v)$, the amplitude is expanded in powers of k^μ . Keeping only the leading term in this expansion leads to the result that $\mathcal{M}[O_+^0(P) \rightarrow X]$ is equal to the amplitude $\mathcal{M}[S^{A+}(P/2)S^{B-}(P/2) \rightarrow X]$ times $\sqrt{2/m_O} \psi(0)$ times a color factor.

For the parton level cross section via gluon gluon fusion we obtain

$$\begin{aligned} \hat{\sigma}[gg \rightarrow O_+^0] &= \frac{9\pi^3 \alpha_s^2 (2m_S)}{2m_S \hat{s}} |\psi(0)|^2 \delta(\hat{s} - m_O^2) \\ \hat{\sigma}[gg \rightarrow O_R^0] &= \hat{\sigma}[gg \rightarrow O_I^0] = \frac{1}{2} \hat{\sigma}[gg \rightarrow O_+^0], \end{aligned} \quad (7)$$

where \hat{s} is partonic center of mass energy squared, and α_s is evaluated at the scale $2m_S$. These expressions must be convolved with parton distribution functions to obtain the total cross sections. To estimate $|\psi(0)|^2$ we use a Coulombic wavefunction with α_s evaluated at the scale $m_S v$,

$$|\psi(0)|^2 = \frac{N_c^3 \alpha_s^3 (m_S v) m_S^3}{8\pi}. \quad (8)$$

This is at best a rough approximation to the actual result. Bound states of superheavy quarks were studied in Ref. [14] using a realistic potential model. These authors showed that the quasi-Coulombic approximation is not very accurate even for superheavy quarkonium. For example, for quarks with masses of 500 GeV, taking $\Lambda_{\text{QCD}} = 200$ MeV, the authors of Ref. [14] find $1/\langle r(1S) \rangle = 25$ GeV for the inverse size of the $1S$ quarkonium state in their potential model, while the Coulombic approximation yields $1/\langle r(1S) \rangle = 35$ GeV. Since $|\psi(0)|^2$ should scale as $\langle r(1S) \rangle^{-3}$, this implies $|\psi(0)|^2$ could be smaller than the quasi-Coulombic estimate by a factor of 2. On the other hand, Ref. [14] also showed that $|\psi(0)|^2$ could be significantly affected by Higgs exchange, which results in an attractive force between superheavy quarks that can increase $|\psi(0)|^2$ by a similar factor. Similar considerations

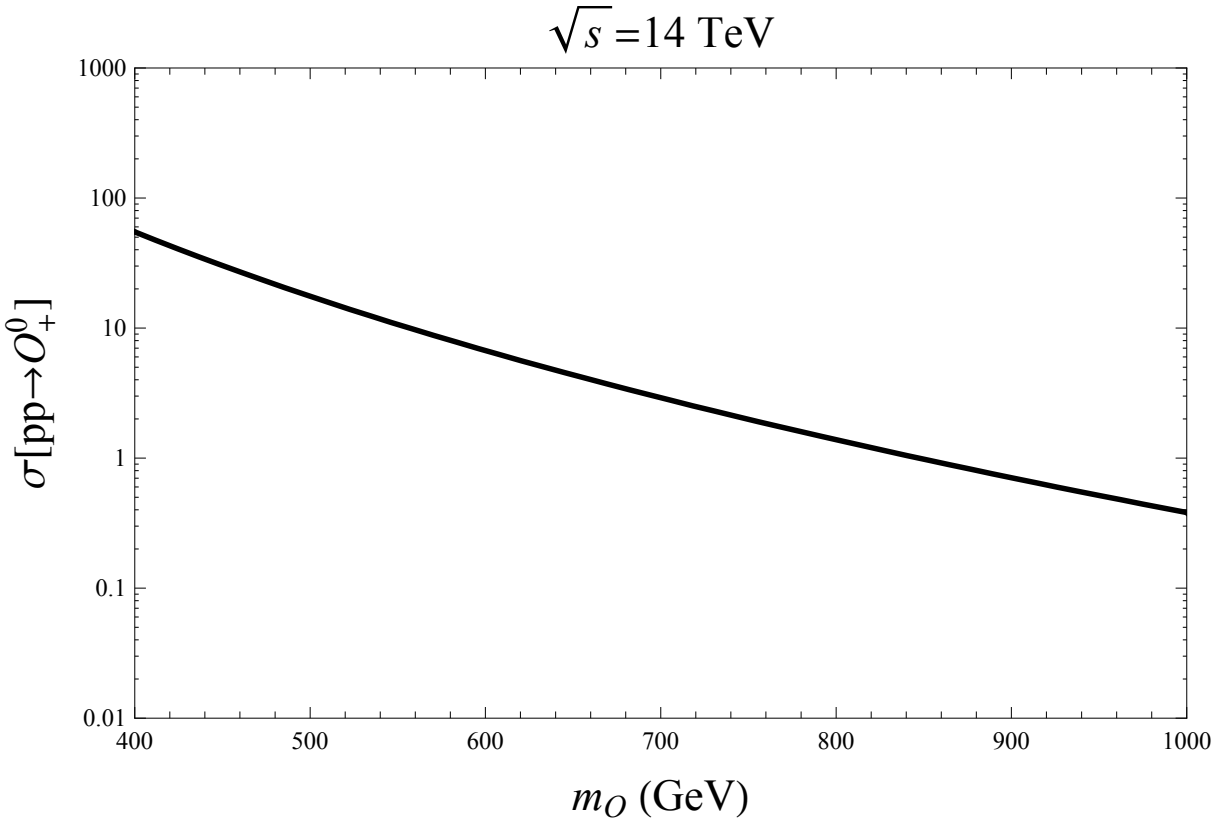


FIG. 1: Total cross section for $pp \rightarrow O_+^0 \rightarrow X$ at the LHC.

hold for color octet scalars, and there is additional uncertainty because the strength of the color-octet couplings to the Higgs is unknown, since the λ_i in Eq. (3) cannot be determined from the octet scalar masses. Furthermore, there are contact interactions from the color-octet scalar potential with unknown coefficients. We expect the quasi-Coulombic estimate to be correct up to factors of order unity.

The total cross section for O_+^0 production at the LHC ($\sqrt{s} = 14 \text{ TeV}$), is shown in Fig. 1. We have used the CTEQ5 parton distribution function [15]. The production cross section ranges from $\sim 50 \text{ pb}$ for $m_{O_+^0} = 400 \text{ GeV}$, to 1 pb for $m_{O_+^0} = 1000 \text{ GeV}$. Cross sections for O_R^0 and O_I^0 are one half as large. With an integrated luminosity of $\sim 100 \text{ fb}^{-1}$ at the LHC, significant numbers of octetonia should be produced if they exist in this mass range.

Next we discuss the two-body decays of octetonia. Unlike the S^A particles, which must decay to Standard Model fermions, the octetonia can decay to Standard Model electroweak gauge bosons. O_+^0 decays to W^+W^- , Z^0Z^0 , $\gamma\gamma$, and γZ^0 , and $O_{R,I}^0$ can decay to W^+W^- and Z^0Z^0 . These channels may be promising for searching for the octetonia since QCD backgrounds are under better control than for final states with four heavy jets. The octetonia can also decay to $t\bar{t}$ and gg and therefore should appear as resonances in dijet and top quark pair production cross sections.

CDF and D0 have done searches for resonances in dijets [16, 17] and $t\bar{t}$ [18, 19] which can be used to rule out new physics coupling to these final states. The upper bounds on $\sigma[p\bar{p} \rightarrow X] \text{ Br}[X \rightarrow t\bar{t}]$ range from about 2 pb for $m_X = 400 \text{ GeV}$ to about 0.5 pb for

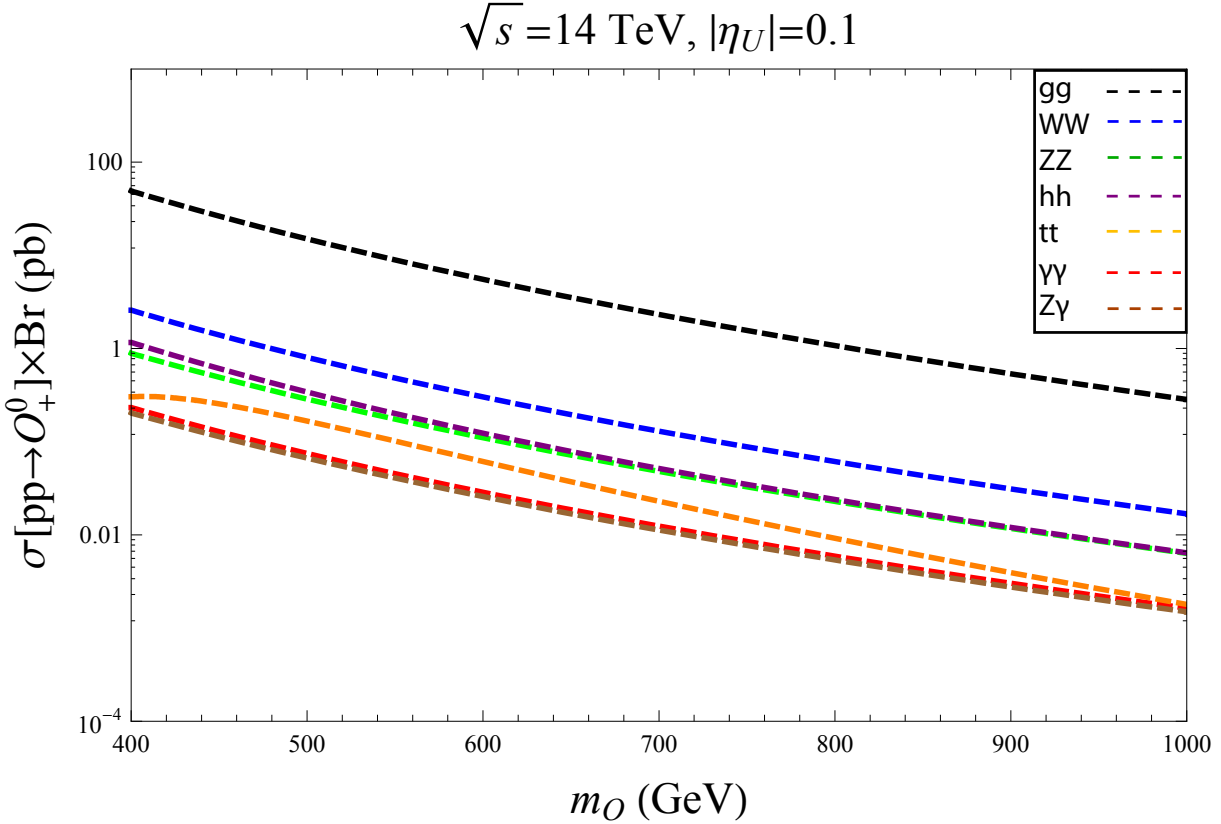


FIG. 2: LHC cross sections for $pp \rightarrow O_+^0 \rightarrow X$, where X is a two-body final state.

$m_X = 900$ GeV. The total cross section for octetonia at the Tevatron is orders of magnitude smaller than these bounds. For example, at $\sqrt{s} = 1.96$ TeV, we estimate $\sigma[p\bar{p} \rightarrow O_+] = 0.062$ pb for $m_{O_+^0} = 400$ GeV and $\sigma[p\bar{p} \rightarrow O_+] = 6.5 \times 10^{-6}$ pb at $m_{O_+^0} = 900$ GeV. The contribution to dijet cross sections from octetonia is also negligible at the Tevatron. The production of octetonia at the Tevatron is suppressed because it is initiated by gluons and because the cross section is proportional to $\alpha_s^2(2m_S)\alpha_s^3(m_S v)$. The gluon rich environment at the LHC will be a much more promising place to search for these states.

Explicit formulae for the two-body decay rates are given in the Appendix A. In Fig. 2 we show the total cross section for O_+^0 times branching fractions for the two-body decay modes. In this plot we choose $|\eta_U| = 0.1$ and $\lambda_1 = 1.0$. In Fig. 3 we show the same cross sections for $|\eta_U| = 0.5$ and $\lambda_1 = 1.0$. The branching fractions for O_+^0 and O_R^0 as a function of m_O are shown in Fig. 4. In the calculations of O_R^0 branching ratios we set $\lambda_1 = \lambda_2 = 1.0$, $\lambda_3 = 0$, $\text{Im } \eta_U \equiv \eta_U^I = 0.0$, and $\text{Re } \eta_U \equiv \eta_U^R = 0.1$ and 0.5 . Branching fractions for O_I^0 are the same as O_R^0 after replacing $\eta_U^R \leftrightarrow \eta_U^I$ and $\lambda_3 \rightarrow -\lambda_3$.

For $|\eta_U| = 0.1$, the annihilation decay $O_+^0 \rightarrow gg$ is the dominant mode for both O_+^0 and O_R^0 . For $|\eta_U| = 0.5$, the decay of O_+^0 is dominated by the non-annihilation decay $O_+^0 \rightarrow \bar{t}\bar{t}bb$, while the dominant decay of O_R^0 is still $O_R^0 \rightarrow gg$, because the decay $O_R^0 \rightarrow \bar{t}\bar{t}tt$ is phase space suppressed for the masses we are considering, while the decays $O_+^0 \rightarrow \bar{t}\bar{t}bb$ and $O_+^0 \rightarrow \bar{b}b\bar{b}b$ are suppressed by m_b^2/m_t^2 and m_b^4/m_t^4 , respectively (assuming that $|\eta_U|$ and $|\eta_D|$ are of comparable magnitude). The total width of O_+^0 and O_R^0 as a function of m_O is shown in

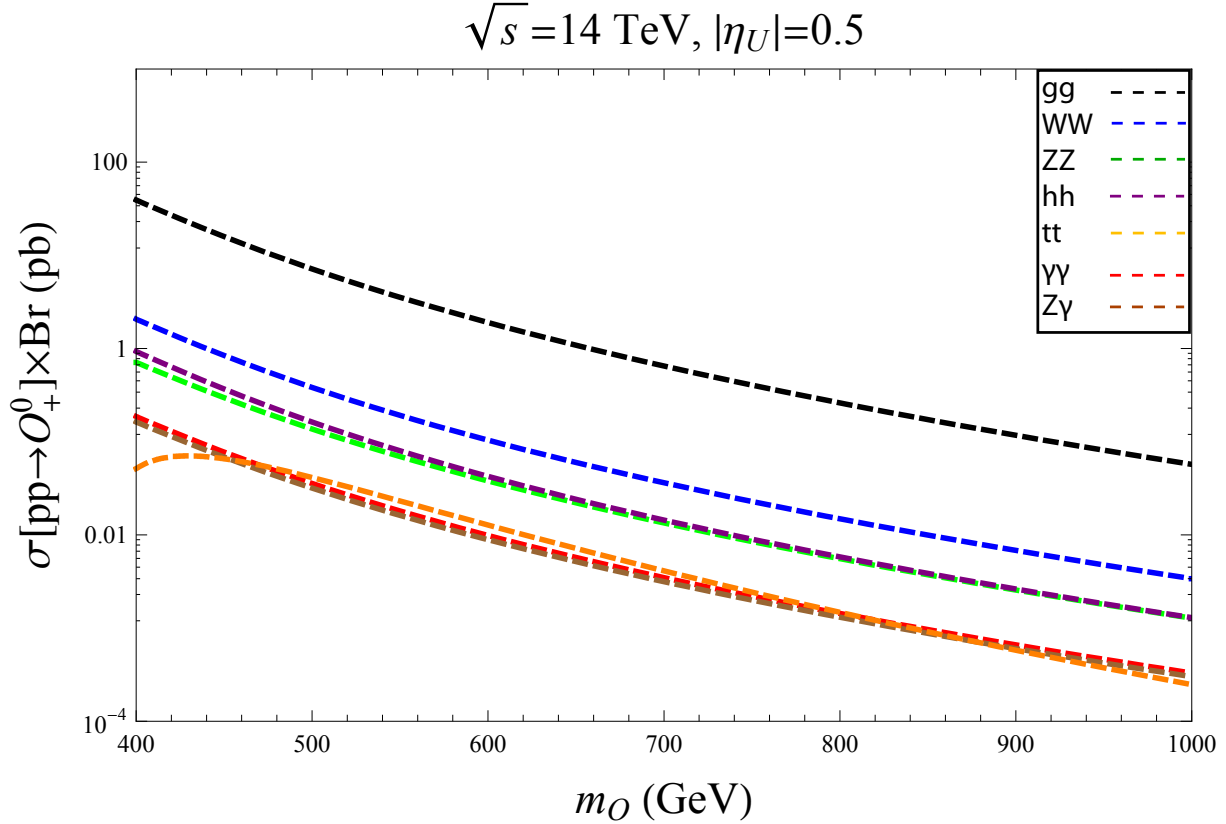


FIG. 3: LHC cross sections for $pp \rightarrow O_+^0 \rightarrow X$, where X is a two-body final state.

Fig. 5, for $|\eta_U| = 0.1, 0.5$, and 1.0 . When the dominant decay channel is gg the widths of the octetonia are less than 1 GeV. When the fall apart decays are dominant, which is the case for $\eta_U = 0.5$ or 1.0 for O_+^0 , the width can be between 1 and 10 GeV depending on $m_{O_+^0}$ and η_U . For O_R^0 the width is always less than 1 GeV below the $t\bar{t}t\bar{t}$ threshold, and between this threshold and 1000 GeV $\Gamma[O_R^0] \lesssim 2$ GeV even for $|\eta_U| = 1.0$.

The next most important decays are to W^+W^- and Z^0Z^0 . For parameters we have chosen in this paper, the branching fraction for $O_+^0 \rightarrow W^+W^-$ is in the range $(0.9-4.1) \times 10^{-2}$ and the branching fraction for $O_+^0 \rightarrow Z^0Z^0$ is in the range $(0.3 - 1.5) \times 10^{-2}$. The branching fraction for two Higgs is about the same as Z^0Z^0 , but this is quite sensitive to the Higgs mass (we have chosen 120 GeV in our calculation) and parameters appearing in the potential. The branching fractions for final states with photons, $\gamma\gamma$ and γZ^0 , are an order of magnitude smaller than W^+W^- . The branching fraction to $t\bar{t}$ is also very sensitive to model parameters. For $|\eta_U| = 0.1$ the branching fraction to $t\bar{t}$ is slightly greater than $\gamma\gamma$ and γZ^0 , while for $|\eta_U| = 0.5$ the $t\bar{t}$ branching fraction is comparable in size. This unusual result is due to an accidental cancellation between the two diagrams contributing to $O_+^0 \rightarrow t\bar{t}$, see Eq. (A9). The pattern of decays for O_R^0 is similar to O_+^0 . The main differences are that fall apart decays to $t\bar{t}t\bar{t}$ are suppressed due to kinematics so other branching fractions are slightly larger, and that decays to $\gamma\gamma$ and γZ^0 are absent because the constituents are electrically neutral.

An important question is whether the peaks in the cross section will be visible above

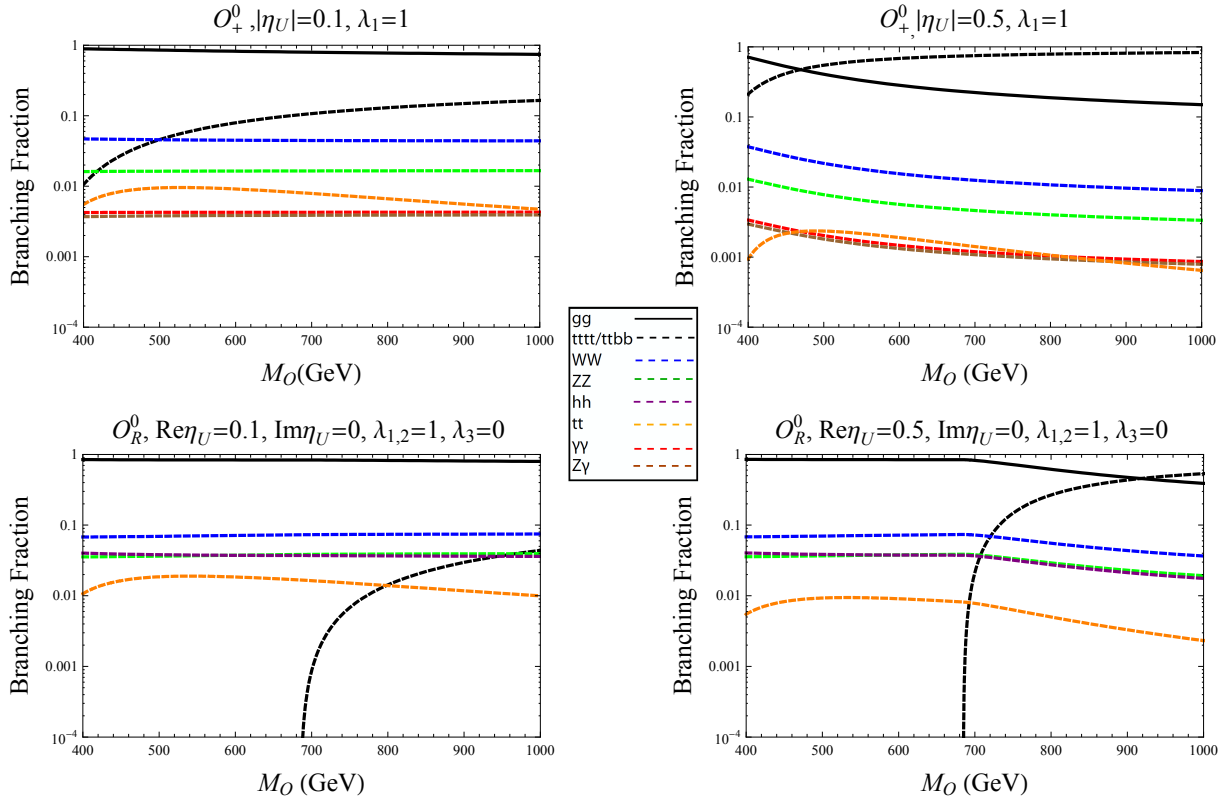


FIG. 4: Branching fractions for $O_{+,R}^0$ two-body decays for $|\eta_U| = 0.1$ and $|\eta_U| = 0.5$.

Standard Model backgrounds for these final states. To test this we consider the process $pp \rightarrow O_+^0 \rightarrow \gamma\gamma$. We calculate $d\sigma/dm_{\gamma\gamma} \times \text{Br}[O_+^0 \rightarrow \gamma\gamma]$, including the width of the O_+^0 which gives this cross section a Breit-Wigner profile. Then we integrate this differential cross section from $m_{\gamma\gamma} - \Delta/2$ to $m_{\gamma\gamma} + \Delta/2$ where Δ is determined by the energy resolution of the measured photon energies. The ATLAS experiment expects to measure photon energies with a resolution of [20]

$$\frac{\Delta E_\gamma}{E_\gamma} = \sqrt{\left(\frac{0.1}{E_\gamma/\text{GeV}}\right)^2 + 0.007^2}.$$

Estimating that $m_{\gamma\gamma} \approx 2E_\gamma$ and $\Delta m_{\gamma\gamma} \approx \sqrt{2}\Delta E_\gamma$ yields $\Delta m_{\gamma\gamma} \approx 2.8$ GeV for $m_{\gamma\gamma} = 400$ GeV and $\Delta m_{\gamma\gamma} \approx 5.9$ GeV for $m_{\gamma\gamma} = 1000$ GeV. For simplicity we will set $\Delta = 6$ GeV. In Table I, $\sigma_{\text{res}}[pp \rightarrow O_+^0 \rightarrow \gamma\gamma]$ is the total cross section for $pp \rightarrow O_+^0 \rightarrow \gamma\gamma$ with $m_{\gamma\gamma}$ within ± 3 GeV of the resonance peak, and $\sigma_{\text{SM}}[pp \rightarrow \gamma\gamma]$ is the leading order Standard Model contribution to $pp \rightarrow \gamma\gamma$ in the same kinematic region. (By leading order we mean the tree level contribution to $q\bar{q} \rightarrow \gamma\gamma$ and the one-loop contribution to $gg \rightarrow \gamma\gamma$ [21].) We impose the cuts $|\eta_{1,2}| < 2.4$, where η_1 and η_2 are the rapidities of the photons in the final state. We consider the case $|\eta_U| = 0.1$ and $|\eta_U| = 0.5$ and find that the contribution from the octetonium resonance equals or exceeds the Standard Model contribution when the octetonium mass is in the 400 to 1000 GeV range. Note that the experimental background also includes background from events with jets that fake photons in the detector. When $m_{\gamma\gamma}$ is in the range 115 GeV to 140 GeV, this background is $(1.25-1.4) \times \sigma_{\text{SM}}[pp \rightarrow \gamma\gamma]$ [22],

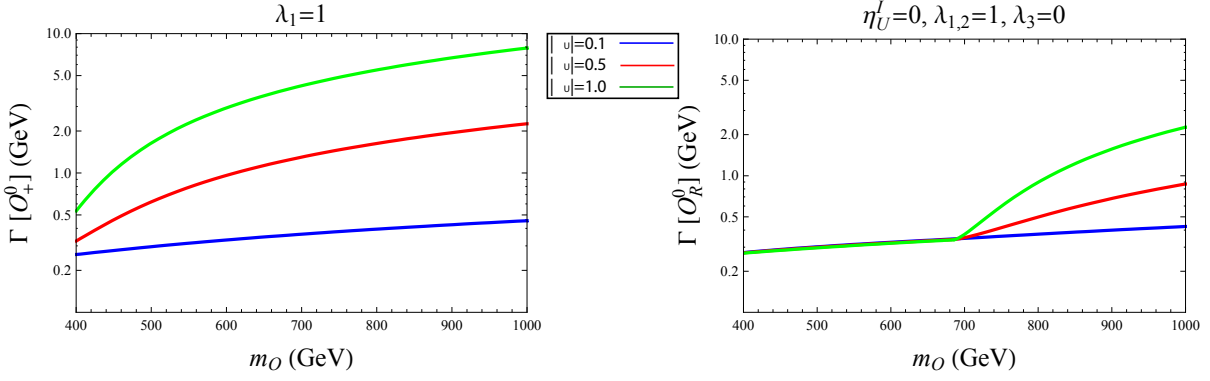


FIG. 5: Total decay widths of $O_{+,R}^0$ for various values of $|\eta_U|$.

	400 GeV	600 GeV	800 GeV	1000 GeV
$\sigma_{\text{res}}[pp \rightarrow O_+^0 \rightarrow \gamma\gamma](\text{fb}), \eta_U = 0.1$	187	24	5.1	1.4
$\sigma_{\text{res}}[pp \rightarrow O_+^0 \rightarrow \gamma\gamma](\text{fb}), \eta_U = 0.5$	149	7.7	1.1	0.23
$\sigma_{\text{SM}}[pp \rightarrow \gamma\gamma](\text{fb})$	12.0	2.2	0.64	0.23

TABLE I: $\sigma_{\text{res}}[pp \rightarrow O_+^0 \rightarrow \gamma\gamma]$ is the resonant cross section for photons with $|\eta| < 2.4$ and $m_{\gamma\gamma}$ within ± 3 GeV of the resonance mass for different values of $m_{O_+^0}$, $\sigma_{\text{SM}}[pp \rightarrow \gamma\gamma]$ is the Standard Model contribution in the same region.

but for larger $m_{\gamma\gamma}$ we expect this background to be smaller. The resonant cross section will still exceed background when $400 \text{ GeV} \leq m_{O_+^0} \leq 1000 \text{ GeV}$ for $|\eta_U| = 0.1$. For $|\eta_U| = 0.5$ the resonant contribution will exceed the estimated background when $400 \text{ GeV} \leq m_{O_+^0} \leq 600 \text{ GeV}$, and possibly for larger $m_{O_+^0}$ depending on the size of the background from jets faking photons at these high energies. These results encourage us to believe that octetonia with masses less than 1 TeV will lead to visible resonances in W^+W^- , Z^0Z^0 , $\gamma\gamma$, and γZ^0 at the LHC. We leave more detailed calculation of the relevant differential cross sections to future work.

To summarize, we have argued that when the Yukawa coupling, η_U , of color octet scalars to Standard Model fermions is less than one, the color octet scalars will live long enough to form color singlet hadrons called octetonia. These hadrons will be visible at the LHC as resonances in W^+W^- , Z^0Z^0 , $\gamma\gamma$, and γZ^0 if the masses of the octetonia are between 400 and 1000 GeV. These channels represent new collider signals for searching for color octet scalars. If no resonances are observed in these channels at the LHC, lower bounds on the masses of color octet scalars can be significantly increased.

Acknowledgments

This work was supported in part by the U.S. Department of Energy under grant numbers DE-FG02-05ER41368 and DE-FG02-05ER41376. We thank Mark Kruse and Ahmad Idilbi

for helpful discussions pertaining to this work. We thank Aneesh Manohar and Al Goshaw for comments on an earlier version of this manuscript.

APPENDIX A: PARTIAL DECAY RATES FOR TWO BODY DECAYS

In this Appendix, we give our results for the partial decay rates for the various two-body decays considered in this paper. For decays to two gluons or photons, there are three diagrams involving vertices with gauge couplings of the S^A to the vector bosons. For two-body decays to gluons we find

$$\Gamma[O_+^0 \rightarrow gg] = |\psi(0)|^2 \frac{18\pi\alpha_s^2(2m_S)}{m_S^2}, \quad (\text{A1})$$

$$\Gamma[O_R^0 \rightarrow gg] = \Gamma[O_I^0 \rightarrow gg] = \frac{1}{2}\Gamma[O_+^0 \rightarrow gg]. \quad (\text{A2})$$

For decays to two photons we find,

$$\Gamma[O_+^0 \rightarrow \gamma\gamma] = |\psi(0)|^2 \frac{16\pi\alpha^2}{m_S^2}. \quad (\text{A3})$$

For decays to W^+W^- and Z^0Z^0 , there are diagrams involving gauge couplings and also a diagram with a virtual Higgs in the S-channel. The contribution from these diagrams depends on the parameters λ_i , $i = 1, 2$, and 3 , appearing in the formulae for the mass terms in Eq. (3). In our numerical calculations we have chosen the Higgs mass to be $m_h = 120$ GeV. For W^+W^- final states we find

$$\begin{aligned} \Gamma[O_+^0 \rightarrow W^+W^-] &= \frac{2|\psi(0)|^2}{\pi m_S^2} \sqrt{1-x_w} \left[m_W^4 G_F^2 \frac{8-8x_w+3x_w^2}{(2-x_w)^2} \right. \\ &\quad \left. + \frac{3\lambda_1 m_W^2 G_F}{4\sqrt{2}} \frac{x_w}{1-x_h/4} + \frac{\lambda_1^2}{128} \frac{4-4x_w+3x_w^2}{(1-x_h/4)^2} \right], \end{aligned} \quad (\text{A4})$$

$$\begin{aligned} \Gamma[O_{R,I}^0 \rightarrow W^+W^-] &= \frac{|\psi(0)|^2}{\pi m_S^2} \sqrt{1-x_w} \left[m_W^4 G_F^2 \frac{8-8x_w+3x_w^2}{(2-x_w)^2} \right. \\ &\quad \left. + \frac{3\lambda_{R,I} m_W^2 G_F}{4\sqrt{2}} \frac{x_w}{1-x_h/4} + \frac{\lambda_{R,I}^2}{128} \frac{4-4x_w+3x_w^2}{(1-x_h/4)^2} \right], \end{aligned} \quad (\text{A5})$$

where $x_w = m_W^2/m_S^2$, $x_h = m_h^2/m_S^2$, and $\lambda_{R,I} \equiv \lambda_1 + \lambda_2 \pm 2\lambda_3$. For Z^0Z^0 final states we obtain

$$\begin{aligned}\Gamma[O_+^0 \rightarrow Z^0Z^0] &= \frac{|\psi(0)|^2}{\pi m_S^2} \sqrt{1-x_z} \left[(1-2s_\theta^2)^4 m_Z^4 G_F^2 \frac{8-8x_z+3x_z^2}{(2-x_z)^2} \right. \\ &\quad \left. + \frac{3(1-2s_\theta^2)^2 m_Z^2 G_F \lambda_1}{4\sqrt{2}} \frac{x_z}{1-x_h/4} + \frac{\lambda_1^2}{128} \frac{4-4x_z+3x_z^2}{(1-x_h/4)^2} \right],\end{aligned}\tag{A6}$$

$$\begin{aligned}\Gamma[O_{R,I}^0 \rightarrow Z^0Z^0] &= \frac{|\psi(0)|^2}{2\pi m_S^2} \sqrt{1-x_z} \left[m_Z^4 G_F^2 \frac{8-8x_z+3x_z^2}{(2-x_z)^2} \right. \\ &\quad \left. + \frac{3m_Z^2 G_F \lambda_{R,I}}{4\sqrt{2}} \frac{x_z}{1-x_h/4} + \frac{\lambda_{R,I}^2}{128} \frac{4-4x_z+3x_z^2}{(1-x_h/4)^2} \right],\end{aligned}\tag{A7}$$

where $x_z = m_Z^2/m_S^2$ and $s_\theta = \sin \theta_W$, where θ_W is the Weinberg angle. Finally, there are decays to γZ^0 which do not receive a contribution from the graph with virtual Higgs. Our result for these decays is

$$\Gamma[O_+^0 \rightarrow \gamma Z^0] = 8\sqrt{2} \alpha G_F |\psi(0)|^2 (1-2s_\theta^2)^2 x_z \left(1 - \frac{x_z}{4}\right). \tag{A8}$$

The octetonia can also decay to $t\bar{t}$ pairs. There is a tree level diagram with two Yukawa couplings from Eq. (1) as well as a graph with virtual S-channel Higgs boson. We find

$$\Gamma[O_+^0 \rightarrow t\bar{t}] = \frac{3}{32\pi} \frac{|\psi(0)|^2}{m_S^2} x_t (1-x_t)^{3/2} \left[\frac{\lambda_1}{1-x_h/4} - \frac{4}{N_c} \frac{|\eta_U|^2}{1-x_t} \frac{m_t^2}{v^2} \right]^2, \tag{A9}$$

$$\begin{aligned}\Gamma[O_{R,I}^0 \rightarrow t\bar{t}] &= \frac{3}{\pi} \frac{|\psi(0)|^2}{m_S^2} x_t (1-x_t)^{3/2} \\ &\quad \times \left[\left(\frac{2(\eta_U^{R,I})^2}{3} \frac{m_t^2}{v^2} - \frac{\lambda_{R,I}}{8(1-x_h)} \right)^2 (1-x_t) + \frac{4(\eta_U^R)^2 (\eta_U^I)^2}{9} \frac{m_t^4}{v^4} \right],\end{aligned}\tag{A10}$$

where $x_t = m_t^2/m_S^2$, $\eta_U^R = \text{Re } \eta_U$, and $\eta_U^I = \text{Im } \eta_U$. Finally, assuming $m_S > m_h$ the octetonia can decay to two Higgs. These proceed by contact interactions which couple two S_A and two Higgs particles. There is also a diagram with S-channel virtual Higgs. The decay rates for octetonia to two Higgs are

$$\Gamma[O_+^0 \rightarrow hh] = \frac{\lambda_1^2}{32\pi} \frac{|\psi(0)|^2}{m_S^2} \frac{(4+2x_h)^2 \sqrt{1-x_h}}{(4-x_h)^2}, \tag{A11}$$

$$\Gamma[O_{R,I}^0 \rightarrow hh] = \frac{\lambda_{R,I}^2}{64\pi} \frac{|\psi(0)|^2}{m_S^2} \frac{(4+2x_h)^2 \sqrt{1-x_h}}{(4-x_h)^2}. \tag{A12}$$

- [1] R. S. Chivukula and H. Georgi, Phys. Lett. B **188**, 99 (1987).
- [2] G. D'Ambrosio, G. F. Giudice, G. Isidori and A. Strumia, Nucl. Phys. B **645**, 155 (2002) [arXiv:hep-ph/0207036].

- [3] A. V. Manohar and M. B. Wise, Phys. Rev. D **74**, 035009 (2006) [arXiv:hep-ph/0606172].
- [4] I. Dorsner and I. Mocioiu, Nucl. Phys. B **796**, 123 (2008) [arXiv:0708.3332 [hep-ph]].
- [5] P. Fileviez Perez, H. Iminniyaz and G. Rodrigo, Phys. Rev. D **78**, 015013 (2008) [arXiv:0803.4156 [hep-ph]].
- [6] P. Fileviez Perez, R. Gavin, T. McElmurry and F. Petriello, Phys. Rev. D **78**, 115017 (2008) [arXiv:0809.2106 [hep-ph]].
- [7] A. V. Povarov, P. Y. Popov and A. D. Smirnov, Phys. Atom. Nucl. **70**, 739 (2007) [Yad. Fiz. **70**, 771 (2007)].
- [8] P. Y. Popov, A. V. Povarov and A. D. Smirnov, Mod. Phys. Lett. A **20**, 3003 (2005) [arXiv:hep-ph/0511149].
- [9] D. Stojkovic, G. D. Starkman and R. Matsuo, Phys. Rev. D **77**, 063006 (2008) [arXiv:hep-ph/0703246].
- [10] M. I. Gresham and M. B. Wise, Phys. Rev. D **76**, 075003 (2007) [arXiv:0706.0909 [hep-ph]].
- [11] M. Gerbush, T. J. Khoo, D. J. Phalen, A. Pierce and D. Tucker-Smith, Phys. Rev. D **77**, 095003 (2008) [arXiv:0710.3133 [hep-ph]].
- [12] CDF collaboration, CDF Note 8954 v1.0.
- [13] M. E. Luke, A. V. Manohar and I. Z. Rothstein, Phys. Rev. D **61**, 074025 (2000) [arXiv:hep-ph/9910209].
- [14] K. Hagiwara, K. Kato, A. D. Martin and C. K. Ng, Nucl. Phys. B **344**, 1 (1990).
- [15] H. L. Lai *et al.* [CTEQ Collaboration], Eur. Phys. J. C **12**, 375 (2000) [arXiv:hep-ph/9903282].
- [16] F. Abe *et al.* [CDF Collaboration], Phys. Rev. D **55**, 5263 (1997) [arXiv:hep-ex/9702004].
- [17] M. P. Giordani [CDF and D0 Collaborations], Eur. Phys. J. C **33**, S785 (2004).
- [18] T. Aaltonen *et al.* [CDF Collaboration], Phys. Rev. Lett. **100**, 231801 (2008) [arXiv:0709.0705 [hep-ex]]; Phys. Rev. D **77**, 051102 (2008) [arXiv:0710.5335 [hep-ex]].
- [19] V. M. Abazov *et al.* [D0 Collaboration], Phys. Lett. B **668**, 98 (2008) [arXiv:0804.3664 [hep-ex]].
- [20] G. Aad *et al.* [ATLAS Collaboration], JINST **3**, S08003 (2008)
- [21] E. L. Berger, E. Braaten and R. D. Field, Nucl. Phys. B **239**, 52 (1984).
- [22] S. Ganjour, arXiv:0809.5163 [hep-ex].